

Journal of Complex Flow

Journal homepage: www.fazpublishing.com/jcf

e-ISSN: 2672-7374



Aerodynamic Effect of a Generic Superbike Winglet by Computational Fluid Dynamics

Muhammad Imran Nor Sani Muhammad¹, Abdulhafid M A Elfaghi^{1,*}

¹ Faculty of Mechanical and Manufacturing Engineering, Universiti Tun Hussein Onn Malaysia, Batu Pahat, 86400, MALAYSIA

*Corresponding Author

Received 24 June 2022; Accepted 4 August 2022; Available online 1 Sept. 2022

Abstract: The research discussing on aerodynamic effect of a generic superbike winglet to prevent loss of speed and control stability. The features of air flow around the winglet were explored in this study, and the magnitude of the drag and lift forces, as well as their coefficient. To determine the forces acting on three distinct types of winglets that have varying angles of attack and are subjected to different velocities, a computational fluid dynamic (CFD) approach is analyzed and simulated using Ansys Fluent. The value of lift and drag forces, as well as their coefficients, were influenced by the angle of attack and velocity. The optimum winglet design should have the lowest drag coefficient and the highest downforce or negative lift force coefficient possible.

Keywords: Heat transfer coefficient, TiO2 nano fluid, nanoparticles, CFD

1. Introduction

An airplane needed a gigantic wing to create the lift force to make its fly while only had a smaller engine. Now, aerodynamic wing on motorcycle do exactly the opposite of wings of airplane, as it creates lift force, wing on motorcycle create downforce which is downward pressure on motorcycle. It is the same you see in car in Formula 1 where there is huge spoiler generally use to push the into racetrack [1-3]. So, we will be doing the same thing on motorcycle to create the downforces. MotoGP bikes really can speed up strongly even at 200 mph. At that speed, wind pressure and aerodynamic drag force on the front of the bikes has taken considerable weight off the front tire and adding the acceleration of the bikes really could lead to instability or even a front-wheel lift-off [4-6]. The presence of winglets on the front of the motorbike can assist in resolving the problem of loss of speed and control stability by creating the downforce toward the motorcycle. To design the best winglet, drag and lift forces must be calculated using CFD simulation [7].

Aerodynamic drag force in general is referred to or described as the resistive force experienced by the object/body when it is in motion with respect to the fluid that surrounds it.

$$F_D = \frac{1}{2}\rho v^2 C_D A \tag{1}$$

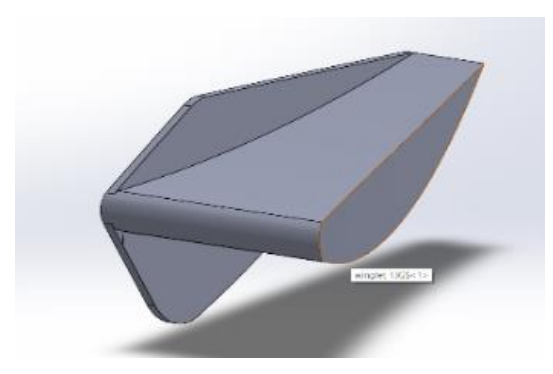
Lift force acting vertically on the body of the vehicle. This force causes the motorcycle's front tire to be lift up in air as applied in the positive direction, whereas it can result in necessary downforce to the front tire if it is applied in negative direction.

$$F_L = \frac{1}{2} \rho v^2 C_L A \tag{2}$$

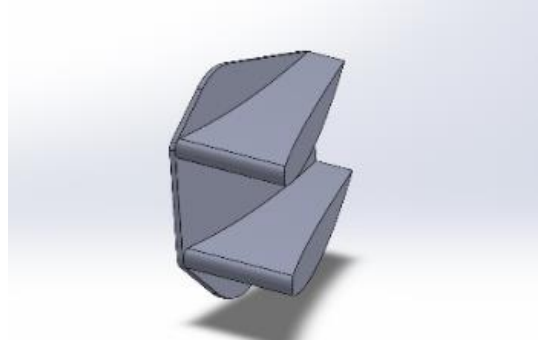
The force that is exerted on to the motorcycle by the aerodynamic properties of the winglet is called the downforce. In fact, this follows Newton's third law [8]. Each action has same and opposite reaction. As a result, the downforce is the opposite force to the lift and is typically stronger [9,10]. Thus, this study will propose an effective numerical model based on the Computational Fluid Dynamics (CFD) approach to obtain the flow structure around a superbike with winglets.

2. Method and Numerical Modelling

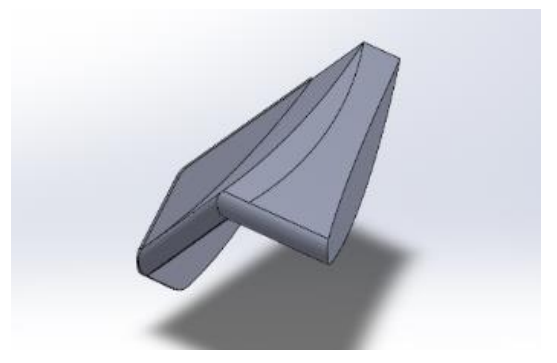
The design of the winglets was constructed by using SolidWork software. Specifications and properties of materials are set in SolidWork as polycarbonate and have a length of 150 mm. Polycarbonate is the toughest plastic, 200 times tougher than glass, and it comes with a lifetime warranty against fracture or cracking. The designed winglets are shown in the following figure 1.



(a) Winglet 1



(b) Winglet 2



(c) Winglet 3

Fig. 1 – Designed of winglets

The topology of the test winglet and grid system is constructed by a commercial package, ICEM/CFD. FLUENT is the CFD solver employed in this study. Using the ANSYS FLUENT, the aerodynamic data and detailed complicated flow structure will be collected and concluded [11,12]. The process starts with the modelling of the winglet and followed by flow field. Then, generate a mesh from the domain and then solve it. Summary of the process shows in figure 2.

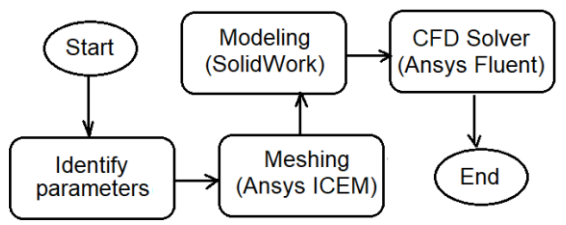


Fig. 2 – Schematics of the workflow

The inlet, outflow, wall, and tool bodies, which is the winglet, are the boundary conditions in the study work. The model has a velocity input and output that is like that of a wind tunnel and is thus referred to as a virtual wind tunnel. After all the surfaces of the wind tunnel have been identified, the numerical solver of ANSYS Fluent would automatically apply the relevant boundary conditions [13].

Table 1 – Condition setup for simulation

Parameter	Variable value	Unit/dimension	
Velocity	36, 80	m/s	
Angle of attack	10, 20	0	
Mesh	0.5	mm	
Turbulent	k-epsilon	Dimensionless	
Density of air	36, 80	kg/m3	

Other than that, the Lift to drag ratio (L/D) has also been utilized to choose the optimal winglet that fulfils the need for higher downforce while reducing drag. For all forms of winglets, the L/D ratio was calculated by dividing the lift coefficient by the drag coefficient.

3. Results and Discussion

The results will be compared in terms of lift and drag force, as well as lift and drag coefficients, C_d and C_l . This project involves 3 types of winglets with different designs. The winglet was simulated at two different angles of attack: 10 degrees and 20 degrees, as well as two different velocities: 36 meters per second and 80 meters per second. Furthermore, the analysis to be assisted by the means of velocity streamline, velocity contour and pressure contour.

3.1 Streamline and velocity contour

The streamline shown in figure 3 represent a flow over the winglet. From the results, it was shows that the velocity at the top of the winglet is higher than the velocity at the bottom of the winglet.

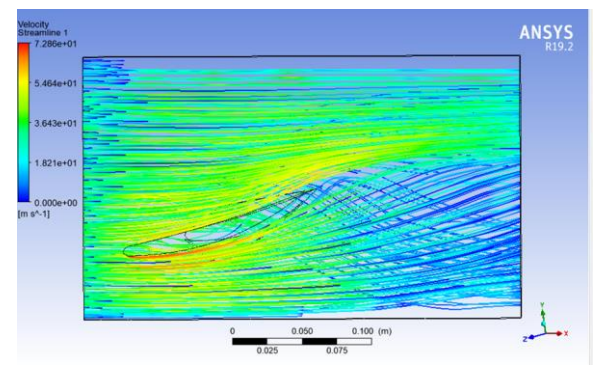


Fig. 3 – Streamline over the winglet

As seen in figure 4, the bottom side of the winglet had a larger portion of the contour in red, indicating the presence of greater velocity, compared to the top side of the winglet, which only had a yellowish color. In fluid mechanics, velocity and pressure are inversely related, so the higher the velocity, the lower the pressure.

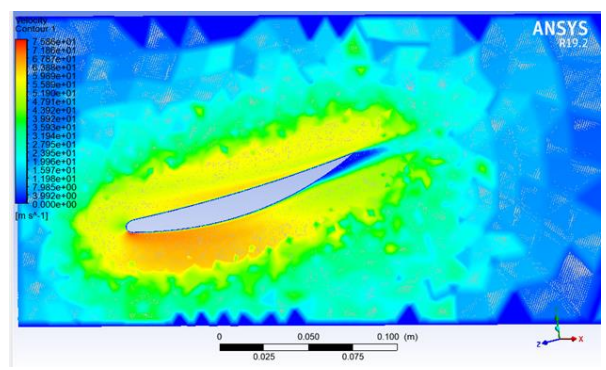
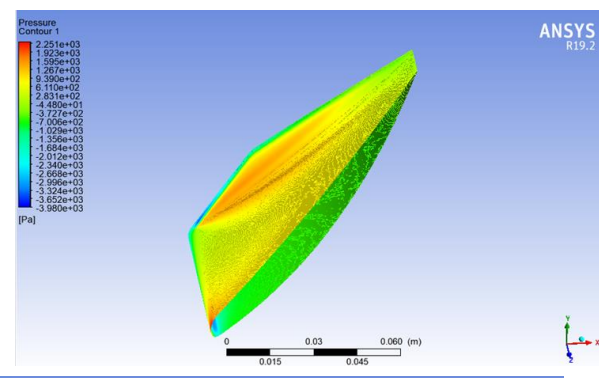


Fig. 4 – Velocity contour

The pressure contour displayed on winglet implies that there is great different in pressure at the top area compared to the bottom area. This is confirmed by the appearance of a reddish-colored pressure distribution on the winglet upper side rather than yellow-colored as shown in figure 5.



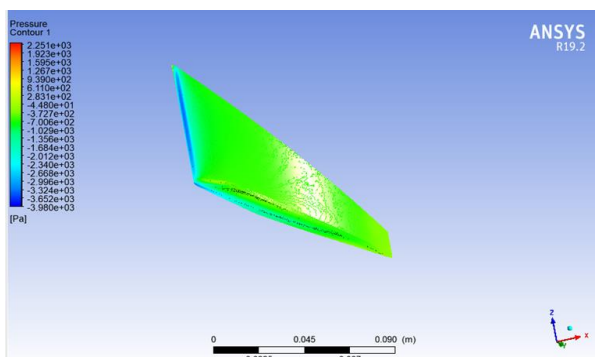


Fig. 5 – Pressure contour at top and bottom surface of the winglet

3.2 Effect of velocity and angle of attack

Table 2 shows the different in negative lift forces, or downforce, between two velocities is great, where the highest of 36 m/s is winglet 3, which is 6.5007N, and the highest of 80 m/s is winglet 2, which is 33.4140N. In term of angle of attack, we can see the difference in negative lift forces, or downforce, between two angle of attack is great, where the highest of 10 degrees is winglet 2, which is 16.56147N, and the highest of 20 degrees also winglet 2, which is 33.4140N. Based on overall observation, as the velocity and angle of attack increase, the negative lift force also increase.

Table 2 – Comparison of velocity and angle of attack on drag force

Winglet	Velocity	10° angle of	20° angle of
	(m/s)	attack	attack
Winglet 1	36	-0.3914 N	-0.2235 N
Winglet 1	80	-2.0407 N	-1.2080 N
Winglet 2	36	-2.8966 N	-2.6595 N
Winglet 2	80	-14.606 N	-13.512 N
Winglet 3	36	0.2183 N	1.5543 N
Winglet 3	80	1.0552 N	7.6101 N

Table 3 was summarized the drag force between two velocities. It shows that the highest of 36 m/s is winglet 3, which is 1.5543N, and the highest of 80 m/s is also winglet 3, which is 7.6101N. In term of angle of attack, the different in drag force between two angles of attack is less compared to winglets 1 and 2, while it is a higher for winglet 3. However, the drag force for the other two winglets, except for winglet 3, is negative, implying that the drag only exists at winglet 3. Based on overall observation, as the velocity and angle of attack increase, the drag force also increase.

Table 3 – Comparison of velocity and angle of attack on drag force

drag force						
Velocity (m/s)	10° angle of attack	20° angle of attack				
36	-0.3914 N	-0.2235 N				
80	-2.0407 N	-1.2080 N				
36	-2.8966 N	-2.6595 N				
80	-14.606 N	-13.512 N				
36	0.2183 N	1.5543 N				
80	1.0552 N	7.6101 N				
	Velocity (m/s) 36 80 36 80 36	Velocity 10° angle of attack 36 -0.3914 N 80 -2.0407 N 36 -2.8966 N 80 -14.606 N 36 0.2183 N				

The parameters that have be picked are 20 degrees of attack and 80 meters per second, based on the comparison that has been done. The L/D ratio is commonly used to represent an airfoil's efficiency. Aircraft with a higher L/D ratio are more efficient than those with a lower L/D ratio. The winglet in our case study resembles an upside-down airfoil. However, due to the presence of negative drag force, we cannot determine which winglet is the best based on the L/D ratio result. As a result of the data, winglet 2 should be the best winglet, as it has the most downforce and the most negative drag force. Finally, winglet 2 generated higher downforce while producing less drag than winglet 1 or 3.

Table 4 – Comparison of lift and drag coefficients

Parameter	Winglet 1	Winglet 2	Winglet 3
Lift force, F_L	-25.7777	-33.4140	-32.2209
Drag force, F_D	-1.2080	-13.5122	7.6101
Lift coefficient, C1	-0.031611	-0.02324	-0.03190
Drag coefficient, C_d	-0.00171	-0.00956	0.00726

4. Conclusion

The bigger the magnitude of velocity, the greater the drag force created, and while the winglet is a priority in terms of downforce, it may only perform properly at a perfect angle of attack. Despite variable drag values, all winglets modified at 10 and 20 degrees were able to create downforce in this testing. Therefore, the data result may imply that winglet 2 at 20 degrees is a preferable option, as it recorded the maximum downforce and lowest drag force

when compared to other winglets, but the result may differ if the winglet position is modified. As a result, it's clear that the angle of attack is a key role in generating more downforce. Downforce is known to provide a variety of benefits, including improved braking and cornering performance as well as increased vehicle traction.

References

- [1] Skorput, P., Mandzuka, S., and Vojvodic, H., "The use of Unmanned Aerial Vehicles for forest fire monitoring." In Proceedings of the 2016 *International Symposium ELMAR*, Zadar, Croatia, 12–14 September 2016: 93–96
- [2] Haris, M.N., Sapit, A., and Mohamed, N.H.N., "Study of Airflow Due to Rear Diffuser of Supercar." *Journal of Complex Flow*, 2(2) (2020): 32-36
- [3] Yomchinda, T., "Simplified Propeller Model for the Study of UAV Aerodynamics using CFD Method." Proceedings of the 5th Asian Conference on Defence Technology, ACDT 2018: 69–74.
- [4] Aref, P., Ghoreyshi, M., Jirasek, A., Satchell, M.J., and Bergeron, K., "Computational Study of Propeller-Wing Aerodynamic Interaction," *Aerospace*, 5(3) (2018): 1–20
- [5] Ali, Mohammad Iqmal Mohd, Azri Nazarain Afandi, and Ahmad Maulan Bardai. "Analysis on Propeller Design for Medium-Sized Drone (DJI Phantom 3)." *International Journal of Innovative Technology and Exploring Engineering*, 8(7) (2019): 217–221.
- [6] Pooneh, A., et al. "Computational Study of Propeller-Wing Aerodynamic Interaction." *Aerospace* 5(3) (2018): 1–20.

Acknowledgement

The authors would also like to thank the Faculty of Mechanical and Manufacturing Engineering, Universiti Tun Hussein Onn Malaysia, and Flow Analysis, Simulation and Turbulence Research Group (FASTREG) for its support.

- [7] M. Rouméas, P. Gilliéron & A. Kourta, "Drag Reduction by Flow Separation Control on a Car After Body." Int. J. Numer. Methods Fluids 60 (2008). ISSN 0271-2091.
- [8] Cheng, K.C., and Fujii, T., "Isaac Newton and Heat Transfer," *Heat Transf. Eng.* 19 (1998): 9–21.
- [9] Musatafa Cakir, "CFD study on aerodynamic effects of a rear wing/ spoiler on a passenger vehicle", submitted to Santa Clara University, December 2012.
- [10] Khosravi, M., Mosaddeghi, F., and Oveisi, M. "Aerodynamic Drag Reduction of Heavy Vehicles using Append Devices by CFD Analysis." J. Cent. South Univ. 22 (2015): 4645–4652
- [11] Yu, W., and Choi, S.U.S., "The Role of Interfacial Layers in the Enhanced Thermal Conductivity of Nanofluids: A Renovated Maxwell Model." *J. Nanoparticle Res.* 5 (2003): 167–171.
- [12] Xuan, Y., and Li, Q., "Heat Transfer Enhancement of Nanofluids." *International Journal of Heat and Fluid Flow*, 21(1) (2000): 58-64,
- [13] E. Baydar and Y. Ozmen, "An experimental and numerical investigation on a confined impinging air jet at high Reynolds numbers," *Appl. Therm. Eng.*, vol. 25, no. 2–3, pp. 409–421, 2005